Valorization of ammonia concentrates from treated urban wastewater using liquid-liquid membrane contactors

E. E. Licon Bernal[a], C. Maya[a], C. Valderrama[a], J.L Cortina[a,b]

[a]Chemical Engineering Department. Universitat Politècnica de Catalunya-Barcelona TECH.

[b]Water Technology Center, CETaqua

*Correspondence should be addressed to: César Valderrama

Departament d'Enginyeria Química, Universitat Politècnica de Catalunya-Barcelona Tech.

Av. Diagonal 647 08028, Barcelona Spain.

Tel.: (+34) 93 4016997

Email: cesar.alberto.valderrama@upc.edu

Abstract

The removal of ammonium from tertiary effluents by zeolites generates basic ammonia concentrates (up to 1-3 gNH_3/L in 1-2 g NaOH/L). This study evaluates the use of hollow fibre liquid-liquid membrane contactors (HFMCs) as a concentration and purification step for ammonia effluents to produce NH_4NO_3 and $(NH_4)_2(HPO_4)$ solutions for potential use as liquid fertilizers. The influence of various operational parameters (i.e., flow rate, initial ammonia concentration and stripping acid concentration) was investigated using a closed-loop setup. Due to the high basicity of the ammonia feed streams (pH >12), the mass transport process was primarily controlled by the free acid concentration in the stripping phase (e.g., HNO_3 and H_3PO_4). A mass transport algorithm to predict the pH of the stripping stream was developed to describe the contactor performance, predict the requirements of the free acid concentration in the stripping phase and optimize the ammonia recovery. Therefore, the closed-loop configuration allowed for ammonia recovery ratios higher than 98% when the required free acid concentration of the stripping phase

was maintained. The exhausted NH_3/NaOH streams after NH_3 removal can be re-used for regeneration of the ammonium-exhausted zeolite filters.

Keywords: Ammonium valorization; Membrane contactor; Hollow fiber; nitrate, phosphate, liquid fertilizers.

1. Introduction

Free ammonia/ammonium that occurs in industrial, farming and domestic wastewater is a major environmental issue because its accumulation in water bodies leads to eutrophication and depletion of oxygen-harming waterborne organisms [1]. Several methods to remove ammonia have been proposed for rich ammonium streams (0.5 to 2 g/L NH_4) (e.g., supernatant liquor of anaerobic digesters (ADs)), ammonia stripping with air at high pH [2], ion exchange [3], magnesium ammonium phosphate precipitation [4] or biological nitrogen elimination [5]. Recently, membrane distillation (MD) and liquid-liquid membrane contactors (LLMCs) have been investigated as an alternative for ammonia removal from AD effluents with a high suspended solid content [6] or directly from a digestion process that treats slaughterhouse waste [7] to reduce the ammonia inhibition during the use of an AD. Although MD possess significant potential for improving NH_3 removal [8,9], the main obstacle in their use with an AD is membrane fouling caused by undegraded organic matter (e.g., proteins and complexes with cations) [10,11]. Fouling reduces membrane hydrophobicity, which hinders ammonia transport and limits scale up of the process [12,13].

For dilute ammonium streams (0.05-0.1 gN-NH_4/L) (e.g., effluents from conventional activated sludge reactors or tertiary treatments), the challenges are related to new legislation requirements to reduce the ammonium discharge levels from regulated values of 15 mgNH_4/L to new recommended values of 1 mgNH_4/L [14]. Ammonium removal treatment processes, such as air

stripping and biological nitrification–denitrification [15], are not economically feasible, and a specific adsorption step is required. Typically, the reduction of ammonium levels below 1 mg/L involves the integration of ion exchange (IX) processes using zeolites [16] where the regeneration step involves generating rich ammonium/ammonia concentrates up to 1-3 g/L in NaCl, NaOH or NaOH/NaCl brines. Because the IX concentration step involves pre-treatment steps including particulate matter removal using sand filters or ultrafiltration processes, the quality of these effluents is more suitable for successful implementation of LLMCs.

MD and hollow fibre membrane contactors (HFMCs) have been proposed as a polishing step to remove low levels of ammonia/ammonium (up to 100 mg-NH_4/L) from industrial effluents [17,18]. HFMCs in PVDF exhibit high ammonia removal efficiencies that are dependent on the feed pH and independent of the ammonia concentration in the feed [19–23]. In comparison to conventional scrubbers, membrane contactors have a much larger specific surface area, and therefore, the space requirements and capital costs are less. In comparison to conventional air stripping processes, LLMCs provide independent control of gas and liquid flow rates without any flooding or foaming and do not require operation at a high-pressure drop [22,24].

Few studies of the removal of ammonia using HFMCs in alkaline solutions have been reported, and in general, these studies are devoted to enhancing the ammonium extraction efficiency in slightly alkaline solutions using sulfuric solutions. The aim of this study was to experimentally study the use of hydrophobic hollow fibre LLMCs as an ammonia separation and concentration step for the production and valorization of ammonium nitrate and diammonium phosphate solutions. A closed-loop experimental configuration was employed using nitric and phosphoric solutions as the stripping solution. The ammonia removal was evaluated from aqueous concentrated streams that were generated during the regeneration step for zeolites used to recover ammonium from a tertiary treatment effluent on a domestic wastewater treatment plant (WWTP). A factorial experimental design was used to determine the influence of the flow rate as

well as the initial ammonia concentration on the overall ammonia mass transport coefficient. In addition, numerical modelling was developed based on the mass transport of ammonia through the membrane contactor, and this model also accounted for pH changes in the stripping solution (details provided in Appendix B). For nitric and phosphoric acid, the effects of the concentration and the nature of the stripping solution on ammonia removal were evaluated.

2. Materials and methods

2.1 Experimental set-up

The experimental set-up is schematically shown in Figure 1. This set-up consisted of a hollow fibre membrane contactor (HFMC) module mounted in a horizontal position, two peristaltic pumps and two tanks of polypropylene (i.e., one for the NH_3/NaOH feed solution and the other one for the nitric or phosphoric acid solution). Clear PVC flexible tubes were employed to connect all of the components. The propylene HFMC module consisted of a Liquid-Cel 2.5x8" Extra Flow X30HF from Membrane–Charlotte (Celgard, USA). The properties of the HFMC are summarized in Table S1 (Supplementary Information) [25].

Figure 1.

The hydrophobic polypropylene (PP) hollow fibre separates both the feed and the stripping circulating phases, and the system works in a closed loop. The ammonia aqueous phase is fed on the lumen side, and the strong acid stripping solution (nitric or phosphoric) is fed on the shell side. An air gap fills the pore of the hydrophobic polypropylene membrane, which is not wetted by the aqueous solutions. In the first step of the removal process, the ammonia gas forms ($NH_{3(g)}$) and diffuses from the bulk of the feed stream to the feed–membrane interface. Then, $NH_{3(g)}$ volatilizes through the feed–membrane interface and diffuses across the air-filled pore of the

membrane. Finally, the gas reacts immediately with the nitric or phosphoric acid at the membrane interface of the shell side.

Initially, deionized water was passed through the module to flush out any trace of the compounds from the previous experiments. The NH_3/NaOH feed solutions were pumped through the lumen side of the hollow fibre membrane contactor at different flow rates, and the stripping acid solution was circulated into the shell side in a countercurrent mode using two peristaltic pumps. Both solutions were recirculated to their respective reservoirs. The volumes of the feed and stripping solutions were 10 and 2 or 3 L, respectively, depending on the experiment requirements. At regular time intervals (10 min), samples (20 mL) were removed from the feed tank to measure the pH and total ammonia concentration. The pH (for solutions between 2 to 12) and acid (nitric or phosphoric) concentration of the receiving tank were monitored by taking samples at specific times. At the end of the experiment, the shell and lumen flows were stopped. The system was cleaned by passing deionized water through both sides to remove the remaining solution. All of the tests were carried out at room temperature (22±1°C). Table 1 summarizes the experimental conditions of these tests.

Three sets of experiments were performed as follows: i) ammonia removal from an aqueous solution with a HFMC and HNO_3 as the stripping solution using a factorial experimental design, ii) ammonia removal with a HFMC in cyclic experiments (addition of ammonia to the feed stream) and HNO_3 as the stripping solution to evaluate the effect of nitric acid neutralization, and iii) ammonia removal from an aqueous solution with a HFMC in cyclic experiments (addition of ammonia to the feed stream) and H_3PO_4 as the stripping solution to evaluate the effect of phosphoric acid neutralization.

2.2 Ammonia solutions

The ammonia synthetic feed solutions simulated the composition of NH_3 and NaOH in concentrated streams generated during the regeneration of zeolites used in the removal of ammonium from treated effluents of a domestic wastewater treatment plant. The feed solutions were prepared using a 10 M NH_3 solution and an 80 g/L NaOH solution. The stripping solutions were prepared by mixing known volumes of 65% (w/w) HNO_3 or 85% (w/w) H_3PO_4 with deionized water. The chemicals were analytical grade reagents (Merck, Spain).

The ammonia feed solutions obtained from elution of ammonium-loaded zeolites with 1.2 g/L NaOH (pH=12.2) were also used. The ammonium solutions were prepared by addition of ammonium chloride powder (NH_4Cl) to domestic tap water. The use of tap water in the preparation of the working solutions was adopted to ensure the presence of competing cations (i.e., sodium, calcium, potassium and magnesium) and anions (i.e., sulfate and bicarbonate) in the solution. The zeolites that were used for ammonium removal from tertiary effluents were natural clinoptinolite, which was provided by Zeocem (Slovakia Republica) as described elsewhere [26,27].

2.3 Experimental procedure: factorial experimental design

The effects of the initial ammonia concentration and flow rate on ammonia recovery were evaluated in a closed-loop batch configuration. The purpose of this factorial design was to serve as a first attempt at predicting the system performance to provide valuable insight for the development of a transport model. The ammonium concentration ranged from 0.5 g/L to 1.7 g/L (with three levels 0.5, 1 and 1.5), and the flow rate ranged from 8 to 10.5 cm^3/s. The NaOH concentration remained constant at 1.2 g/L based on the zeolite regeneration protocol. The HNO_3 or H_3PO_4 concentrations of the stripping phase were fixed at 0.4 M and 0.5 M, respectively, taking into account the recommendations of the membrane provider for the chemical stability of the HFMC.

The effects of the total initial ammonia concentration and flow rate on ammonia recovery using HNO_3 as the stripping solution were studied using a central composite design with a factorial part 2^k, a central point (n_o) and two axial points at the axis corresponding to each factor and situated a distance (α) from the central point. Then, the number of points was calculated according to Eq. 1:

$$N = 2^k + 2k + n_0 \quad (1)$$

The central composite design has circular symmetry around a central point and requires 5 levels for each factor, which allows for increasing resolution with a reasonable number of experiments. In addition, this design is suitable for estimating the curvature of a response in a well-defined region of variables. The levels of the concentration and flow rate were established based on the module limits (i.e., flow rate and ranges of ammonia concentration) that are typically obtained from the elution of loaded zeolites.

For simplicity, the variables were coded, and the conversion between the coded variable and its actual value was calculated by Eq. 2:

$$X^*_i = \left\{\frac{X_i(X_{i\,Sup}+X_{i\,low})}{X_{i\,Sup}-X_{i\,low}}\right\} \quad (2)$$

where X^*_i, and x_i are the coded and real value of variable i, respectively. $X_{i,Sup}$ and $X_{i,low}$ are the upper and lower levels from the factorial design, respectively.

Therefore, for the two factor levels (values of 1 and -1) using this encoding rule, the axial points are α = 1.414 with a centre point value of 0. In addition, the total number of experiments was 9 (Table 1). The centre points (Exp.9 in Table 1) were performed in triplicate to identify the process instability.

Experiment	**Feed stream** C_0 **(mg** NH_3**/L)**	**Stripping stream** C_0 **(**HNO_3**) (M)**	**Q(**cm^3/s**)**	X^*_{C0}	X^*_Q
1	500	0.5	8.05	-1	-1
2	1500	0.5	8.05	1	-1
3	500	0.5	10.5	-1	1
4	1500	0.5	10.5	1	1

5	292.9	0.5	9.16	-1.414	0
6	1707.1	0.5	9.16	1.414	0
7	1000	0.5	7.59	0	-1.414
8	1000	0.5	11.055	0	1.414
9	1000	0.5	9.16	0	0

Table 1. Details of the factorial experimental design for the ammonia concentration using the HFMC with a 1.2 g/L NaOH background feed composition and a 0.5 M HNO_3 stripping stream.

The surface response for ammonia removal was determined using Eq. 3:

$$Y = \beta_0 + \sum_{i=1}^{k} \beta_i X_i + \sum_{i=1}^{k} \beta_{ii} {X_i}^2 + \sum_{\substack{i,j \\ i<j}}^{k} \beta_{ij} X_i X_j + \varepsilon \quad (3)$$

where Y is the response surface, Xi is the variable vector, B_0, B_i, B_{ii} and B_{ij} are the regression coefficients and ε is the error function.

2.3 Analytical methods

NH_3 was potentiometrically determined using an ammonia ion selective electrode (4500-NH3 D). A Hach 51927 ammonia gas-sensing gas combination electrode was used for this purpose. The ion concentrations were determined using an Ionic Chromatograph (Dionex ICS-1100 and ICS-1000 Thermo Fisher Scientific, USA). The pH of the samples, which ranged between 2 to 12, was measured with a pH meter (pH meter GLP22 Crison, Spain). For strongly acidic (pH<2) and strongly basic solutions (pH>12), where the pH could not be accurately measured by the pH glass electrode, proton and hydroxide concentrations were determined by potentiometric titration. 0.1 M NaOH and 0.1 M 0.1 M HCl solutions were used.

3. Ammonia recovery as ammonium nitrate and diammonium phosphate by the HFMC: removal mechanism and model description

The mechanism of ammonia removal from the feed solution (zeolite regeneration concentrates at pH>12) in a HFMC is shown in Figure 2. At pH>12, the global process of extraction and conversion to ammonium nitrate and phosphate salts is described by Eqs. 4-8:

$$NH_{3f} = NH_{3(g)f} \quad (4)$$

$$NH_{3(g)f} \leftrightarrow NH_3(g)_{mf} \quad (5)$$

$$NH_3(g)_{ms} \leftrightarrow NH_3(g)_s \quad (6)$$

$$NH_3(g)_s + HNO_3 \leftrightarrow NH_4NO_3 \quad \text{(for } HNO_3 \text{ as stripping solution)} \quad (7)$$

$$2NH_{3s} + H_3PO_4 \leftrightarrow (NH_4)_2HPO_4 \quad \text{(for } H_3PO_4 \text{ as stripping solution)} \quad (8)$$

where the sub-indices f, m and s indicate the feed, membrane and stripping phases, respectively. However, for a feed stream with strongly basic conditions, the mass transfer of NH_{3f} was only affected by the free acid concentration of the stripping phase and controlled by the neutralization reactions (7-8). Therefore, the free acid concentration in the stripping compartment was the primary driving force for enhancing the ammonia removal from the feed solution.

Figure 2.

The ammonia-receiving solution consists of a strong acid solution that reacts with the transported ammonia. Therefore, the free proton concentration gradually decreases until the acid (HNO_3 or H_3PO_4) is completely neutralized. The free proton concentration (A detailed description is provided in Appendix A) along the transport process was predicted using the mass balance, the acid-base equilibrium constants and the electric neutrality equation.

A numerical algorithm to describe the ammonium removal processes on the hollow fibre membrane contactor module was developed (Eqs. 3A and 7A) that incorporated the influence of

the chemical equilibrium in the acid collector, as is described in Appendix B (A more detailed description is provided in the Supporting Information). This algorithm was designed to estimate a) the experimental conditions to obtain target ammonium removal ratios or the ammonium salt (NH_4NO_3 and $(NH_4)_2HPO_4$)) concentrations in the stripping phase. In addition, b) the feed pH variation on the stripping stream due to the conversion of ammonia to ammonium salts was also incorporated by means of the acid-base reactions.

Determination of the ammonia mass transfer coefficient ($K_{m(NH_3)}$)

The ammonia flux (J_{NH_3} (mol.m^{-2}s^{-1}) through the membrane was controlled by the ammonia partial pressure difference between the feed and the stripping streams ($p_{NH3,f} - p_{NH3,s}$) and the overall mass transfer coefficient ($K_{m(NH_3)}$), as described by Equation 19:

$$J_{NH3} = \frac{K_{m(NH3)}(p_{NH3,f} - p_{NH3,s})}{RT} \quad (9)$$

Assuming that the ammonia partial pressure is directly proportional to the ammonia concentration and taking into account that the pH of the feed stream remained constant during the experimental run (ΔpH<0.1), the ammonia concentration is proportional to the total ammoniacal concentration ($C_{t(N)}$) in the feed. In the stripping stream, the acidity was maintained to ensure that the total ammoniacal nitrogen will be in the ammonium form (>99%). The ammonia partial pressure of the stripping stream can be considered a very small value. Under this hypothesis and taking into account the total ammonium/ammonia mass balance and Eq. 9, $K_{m(NH3)}$ (m/s) can be experimentally determined using Eq. 10 [19]:

$$\ln \frac{C_{o(NH3)f}}{C_{t(NH3)f}} = \frac{K_{m(NH3)} A_m}{V_f} t \quad (10)$$

where V_f is the total volume of the feed solution (L), A_m is the membrane module area (m^2) and $C_{o(NH3)f}$ and $C_{t(NH3)f}$ are the free ammonia concentrations in the feed stream at t=0 and time t, respectively. If a linear relationship is obtained by plotting $\ln(C_{o(NH3f)}/ C_{t(NH3f)})$ as a function of time, $K_{m(NH3)}$ can be calculated from the slope ($K_{m(NH3)}A_m/V_f$).

4. Results and discussion

4.1. Recovery of ammonium using HNO_3 as the stripping solution: concentration and flow rate influence

The variation in the logarithm of the ammonia concentration (Ln $C_{t(NH3)}/C_{0(NH3)}$) as a function of the filtration time of the feed solutions (experimental design Table 1) is shown in Figure 3.

Figure 3.

The NH_3 removal process is very fast with more than 80% removal occurring in less than 30 minutes, and the ammonia flux decreased as the membrane filtration time increased because the reduction in the ammonia concentration gradient implies a decrease in the partial pressure gradient (Eq. S15). The concentration ratio decreased with a typical decay behaviour, which is predicted by the ammonia transport model (Appendix B).

The $K_{m(NH3)}$ values ranged from 0.2 to 0.6 10^{-5} m/s and were comparable to published values for similar HFMC modules with hydrophobic PP and polyvinylidene fluoride (PVDF) capillary membranes, which are provided in the Supplementary Information (Table S2).

The mass transfer coefficients using HNO_3 were on average $0.4x10^{-5}$ m/s even though the absolute mass transfer did not vary substantially as a function of the initial ammonia concentration (0.8 to 1.7 g/L). The $K_{m(NH3)}$ values were similar to those reported for a synthetic solution at a similar feed pH (11 to 13) using PP [19,22] or PVDF [25]. Ashrafizadeh and Khorasani [27] and Zhu et al. [23] used pure NH_4Cl solutions, and the observed transfer coefficient was independent from the ammonia concentration.

Moreover, Waeger and Fuchs [6] and Lauterbock et al. [9] conducted studies using PP membranes and temperatures between 20 and 40ºC at pH values of 8.6 to 10 with anaerobic

digestates, and the measured $K_{m(NH3)}$ values were dependent on the free ammonia concentration. Zhu et al. [19] also reported similar results using viscous media with volatile compounds.

Data analysis of the ammonia K_m values for the factorial design (Table 1) indicated correlation with the initial ammonia concentration (C_0) and flow rate (Q) as defined by Eq. 11:

$$K_m * 10^6 = 3.028 - 0.662X^*_{C_0} + 0.929\, X^*_Q + 0.27\, {X^*_{C_0}}^2 + 0.797\, {X^*_Q}^2 - 0.17\, X^*_{C_0} X^*_Q \quad (11)$$

where the error between the experimental and estimated K_m values was calculated using Eq. 12:

$$error(\%) = \left(\frac{|K_{m,exp} - K_m|}{K_{m,exp}}\right) * 100 \quad (12)$$

The experimental and predicted ammonia removal amounts as well as the error estimated for each experiment are listed in Table S3. The reported errors were used to estimate the mean deviation (by averaging all values), which was approximately of 4.6%. This deviation indicated that the regression equation provided a suitable fit to the system performance.

The measured and predicted values were used to plot the ammonia overall mass transport coefficient (K_m) response surface as a function of the two main operation variables (i.e., the initial ammonia concentration and flow rate on the HFMC module), as is shown in Figure 4.

Figure 4.

The pH (12.2±0.3) of the feed stream (data not shown) remained constant during the experiment as the buffer capacity of the background NaOH solution (1.2 g/L NaOH) buffered the change in the pH due to the transfer of NH_3 from the feed to the stripping stream. The treated solutions containing between 15 and 150 mgNH_3/L are suitable for re-use as elution solutions for ammonium removal filters based on zeolite adsorbents.

4.2 Evaluation of the recovery of ammonia as ammonium nitrate in the stripping phase: influence of free acid concentration

To produce ammonium nitrate, consecutive extraction experiments were performed. The variation in the total ammonium concentration and pH of the stripping solution as a function of time for two consecutive experiments are plotted in Figure 5. In the first cycle, after the ammonium concentration decreased from 1700 to 20 mg NH_3/L (98% removal), the pH of the 0.5 M HNO_3 stripping solution was 0.3, which was reduced to values of 0.8 due to the neutralization reaction defined in Eq. 3A. However, at the end of the first cycle (approximately 80 minutes) (e.g., R(%) = 99%), a new fresh NH_3 solution (1700 mgNH_3/L) was introduced into the feed stream.

Figure 5.

During the second cycle (from 80 to 120 min), the reduction of NH_3 follows the typical exponential decay but it stabilized at approximately 800 mgNH_3/L (C/C_0= 0.5 or R(%)= 50%). During the second cycle, the acidity decreased from an initial pH value of 0.8 to 8 when the ammonia transfer stopped because the NH_3 concentration in the feed phase remained constant over time. At this moment, the free acid concentration of the stripping phase was not sufficient to promote ammonia transfer through the membrane phase. Therefore, this concentration decreased due to the partial pressure of NH_3, as shown in the equilibrium in Eq. 1A.

A theoretical description of the development of the ammonia mass transport description code is included in Appendix B. This code was used to predict the free ammonia concentration in the feed and stripping phase as well as the pH of the stripping phase, which are plotted as solid lines in Figure 5. The modelling parameters that are related to the membrane transport properties are summarized in the Supplementary Information (Table S1).

The predicted free ammonia concentrations in the feed solutions are well described by the model, and the prediction error between the experimental and predicted values was less than 5%. The transport code also calculated the free concentration in the stripping phase with values less than 0.1 mgNH_3/L at a pH less than 2. The reduction in the free acid concentration (H^+) below 0.01 M

represented the increase in the free ammonia concentration in the stripping phase because the neutralization reaction (Eq. 7) is not favoured. In addition, the variation in the pH of the stripping phase was calculated and measured, and the predicted values exhibited differences in the pH below 0.2, except for the values corresponding to non-buffered solutions with stoichiometric ratios for nitric and ammonia (pH=4 to 8). Then, the variation in the pH of the stripping is well predicted by Eq. 3A and can be used to control the process of ammonium nitrate salt production for use as liquid fertilizers.

Finally, the increase in the ammonium nitrate concentration of the stripping phase as a function of time for both the experimental (points) and predicted (solid lines) results are shown in Figure 5. After two cycles, 9 g/L NH_4NO_3 (c.a. 1% (w/w) NH_4NO_3) was produced for a feed tank volume/stripping tank volume ratio of 5. The model provides a good prediction of the total ammonium nitrate concentration in the stripping phase with a prediction error less than 5%.

4.3 Evaluation of ammonia recovery as diammonium phosphate in the stripping phase: influence of phosphoric free acid concentration.

Because diammonium phosphate solutions are widely used as liquid fertilizers, the substitution of nitric acid with phosphoric acid as the stripping phase was evaluated. Because phosphoric acid has a relatively lower strength compared to that of nitric acid, the measured ammonia removal profiles were different from those observed for nitric acid.

The variation in the total ammonia concentration and pH of the stripping solution as a function of time for two consecutive cycles is plotted in Figure 6. In the first cycle, after the ammonium concentration decreased from 1760 to 105 mgNH_3/L (94% removal), the pH of the 0.4 M H_3PO_4 stripping solution, which was 1, decreased. The pH values followed a typical neutralization S-shaped function to achieve stabilization (approx. at pH = 7) due to the neutralization reaction,

which occurs in two steps according to the acid-base properties of H_3PO_4, as defined in Eqs. 13 and 14.

$$NH_{3s} + H_3PO_4 \leftrightarrow NH_4H_2PO_4 \quad (13)$$

$$NH_4H_2PO_4 + NH_3 \leftrightarrow (NH_4)_2HPO_4 \quad (14)$$

During the cycle, the driving force, which is the difference between the ammonia vapour pressures on both sides of the fibre, was achieved by the fast reaction that occurred at the gas/liquid phosphoric interface. For a given number of moles of ammonia transported, an equal number of H_3PO_4 moles was converted to $H_2PO_4^-$. The theoretical pH was calculated using Eq. 7A and provided a good prediction of the measured values, as shown in Figure 6.

However, at the end of the first removal cycle (approx. 80 minutes) (e.g., R(%) = 93%), a fresh solution of NH_3 (1760 mgNH_3/L) was introduced into the feed stream.

The initial pH (12.2.±0.3) of the feed stream remained constant, and the evolution of the concentration ratio (C_t/C_0) followed a trend that was similar to that for HNO_3, confirming that for a given flow rate and initial concentration, the removal was only dependent on the fast reaction on the stripping side. This reaction is only affected by the excess strong acid (nitric or phosphoric). The removal process is very efficient, and in less than 30 minutes, the ammonia in the feed is less than 20% of the initial concentration. The membrane mass transfer coefficient for $NH_{3(g)}$ ($k_{j,g,pore}$ = 4.06 × 10^{-4} (m/s)) (Supplementary Information) is the proportionality constant between the difference in the partial pressures on each side of the membrane and the mass flux which decreased with time due to the decrease in the ammonia concentration gradient.

Figure 6.

During the second cycle (from 80 to 140 min), the NH_3 concentration was stabilized at approximately 1060 mgNH_3/L (C/C_0= 0.6). Along the second cycle, the acidity decreased from an

initial pH of approximately 7 for a solution containing a mixture of $(NH_4)H_2PO_4/(NH_4)_2HPO_4$ to a pH of 9 with a solution containing $(NH_4)_2HPO_4$ at this stage. Then, the ammonia transfer stopped because the NH_3 concentration in the feed phase remained constant over time, which followed the same trend as that observed with nitric acid.

The predicted concentrations of free ammonia in the feed solutions are described well by the model based on the error between the measured and estimated values being less than 5%. The free concentration of the stripping phase was also calculated to be less than 0.001 $mgNH_3/L$ when the pH values were less than 7 (Figure 6). The decrease in the free acid concentration to less than 10^{-3} mol/L represented an increase in the free ammonia concentration in the stripping phase because the neutralization reactions (Eqs. 13-14) are not favoured. In addition, the variation in the pH of the stripping phase was calculated and measured, and the predicted values exhibited differences less than 0.2 units, except for the values corresponding to the buffered solutions with stoichiometric ratios of $(NH_4)H_2PO_4$ /$(NH_4)_2HPO_4$ (pH=6 to 7). Then, the variation in the pH of the stripping phase was predicted well by Eq. 3A and can be used to control the production process for diammonium phosphate salts.

The second cycle starts with a fresh solution of NH_3 (1.76 g/L) and also exhibits typical exponential decay for stabilization at a value of approximately 13 g/L. The evolution of the pH follows an S-shaped function and reached a value of 9 after stabilization, corresponding to the stabilization of ammonium removal. When a certain number of moles of ammonia are transported, the $H_2PO_4^-$ species are quantitatively converted to HPO_4^{2-} according to Eq. 7A, and then, $(NH_4)H_2PO_4$ is converted to $(NH_4)_2HPO_4$. In addition, the pH of the expected solution can be calculated by taking account a mixture of NH_4^+ and $H_2PO_4^-$ species. The pH of this solution was predicted using Eq. 7A, and an overestimation of the pH values was observed, as shown in Figure 6 (errors were between 10-15%). This result indicated that additional effort is required with a focus on the ammonia mass transfer properties in insufficiently strong acidic solutions.

Finally, the increase in the ammonium phosphate concentration in the stripping phase as a function of time for both the experimental (points) and predicted (solid lines) results are shown in Figure 6. After two cycles, 9 g/L $(NH_4)_2HPO_4$ (c.a. 0.9% (w/w) $(NH_4)_2HPO_4$) were produced for a feed tank volume/stripping tank volume ratio of 5. The model provided a good prediction of the total ammonium phosphate concentration in the stripping phase with an error less than 5%.

The final concentration achieved using nitric and phosphoric acid as the stripping solution was one order of magnitude less than that obtained using a 10% (w/w) content of commercialized liquid fertilizers. However, the addition of free nitric/phosphoric acid to the stripping stream could be repeated if higher concentrations of salt are needed for direct agronomical applications. This solution if often used to produce diammonium-phosphate fertilizers from ammonium that is present in waste effluents, which is free of inorganic and organic solution components. Then, the recovery systems can reduce the levels of both the inorganic and organic contaminants due to its transport through the liquid-liquid contactor being impossible because only species in the gas form can be transport through the hollow fibres. Therefore, this fertilizer raw material or fertilizer itself can achieve the quality requirements of the fertilizer industry.

4.4 Ammonium from loaded zeolite desorption step using phosphoric acid: performance of a HFMC in consecutive cycles

The contactor performance for ammonia recovery using phosphoric acid was evaluated using excess acid in the stripping solution (see Figure 6). The solutions obtained from elution of the ammonium-saturated zeolites were loaded using tertiary effluents from a WWTP and 1.2 g/L NaOH solutions [27]. The concentration of the ammonia solutions that were obtained from four cycles ranged from 1.8 to 2.7 g NH_3/L. These solutions were fed into the closed-loop

configuration, resulting in recoveries of 93 to 98%, as shown in Figure 7. The variation in the diammonium phosphate solution in the stripping phase increased to 10 to 14 g/L.

Figure 7.

A progressive decrease in the residual concentration was correlated to a decrease in the mass transfer coefficients from 0.82 (cycle 1) to 0.54 (cycle 4) 10^{-5} m/s. Although excess strong acid (H_3PO_4) was present during the first cycle, the dominant acid species in the second cycle was $H_2PO_4^-$, which is a weak electrolyte.

5. Conclusions

Studies with an HFMC using nitric and phosphoric acid as the stripping solution resulted in an ammonia recovery capacity higher than 95-98% when free acid is present in the stripping phase. This result is consistent with previously reported values using H_2SO_4 and HCl (i.e., removal efficiency higher than 95%).

The produced ammonium salts were highly pure because only gaseous species can be transported through the hydrophobic membrane. The predictive model proposed in this study was able to describe the ammonia removal process with minimal deviations from the experimental data. More rigorous approaches will be considered in future studies, where the model will include the solution for the hydrodynamics inside the shell side and account for non-ideal solutions.

Based on the absence of metal ions or organic micropollutants (e.g., potentially incorporated during the zeolite adsorption-elution step), the quality of the by-products is high because their transport on the HFMC is restricted by the membrane properties. After removal of NH_3, the exhausted NH_3/NaOH streams can be re-used for regeneration of the ammonium-exhausted zeolite filters.

Acknowledgments

This research was supported by the ZERO-DISCHARGE project (CTQ2011-26799) and Waste2Product project (CTM2014-57302-R) financed by the Ministerio de Economía y Competitividad (MINECO) and the Catalan Government (Project Ref. 2014SGR50). The National Council of Science and Technology of Mexico (CONACYT) supported the work of Edxon Eduardo Licon Bernal within the scope of fellowship reg: 213775. Authors acknowledge Membrane–Celgard Co, (Charlotte, USA) for samples supply.

References

[1] P.F. Atkins, D.A. Scherger, Review of physical-chemical methods for nitrogen removal from wastewaters., Progr. Water Technol. 8 (1975) 713–720.

[2] C. Resch, A. Wörl, R. Waltenberger, R. Braun, R. Kirchmayr, Enhancement options for the utilisation of nitrogen rich animal by-products in anaerobic digestion., Bioresour. Technol. 102 (2011) 2503–10. doi:10.1016/j.biortech.2010.11.044.

[3] T. Wirthensohn, F. Waeger, L. Jelinek, W. Fuchs, Ammonium removal from anaerobic digester effluent by ion exchange., Water Sci. Technol. 60 (2009) 201–10. doi:10.2166/wst.2009.317.

[4] J.D. Doyle, S.A. Parsons, Struvite formation, control and recovery, Water Res. 36 (2002) 3925–3940. doi:10.1016/S0043-1354(02)00126-4.

[5] M.J. Rothrock, A.A. Szögi, M.B. Vanotti, Recovery of ammonia from poultry litter using flat gas permeable membranes., Waste Manag. 33 (2013) 1531–8. doi:10.1016/j.wasman.2013.03.011.

[6] F. Wäeger-Baumann, W. Fuchs, The Application of Membrane Contactors for the Removal of Ammonium from Anaerobic Digester Effluent, Sep. Sci. Technol. 47 (2012) 1436–1442. doi:10.1080/01496395.2011.653468.

[7] B. Lauterböck, M. Ortner, R. Haider, W. Fuchs, Counteracting ammonia inhibition in anaerobic digestion by removal with a hollow fiber membrane contactor., Water Res. 46 (2012) 4861–9. doi:10.1016/j.watres.2012.05.022.

[8] B. Lauterböck, K. Moder, T. Germ, W. Fuchs, Impact of characteristic membrane parameters on the transfer rate of ammonia in membrane contactor application, Sep.

Purif. Technol. 116 (2013) 327–334. doi:10.1016/j.seppur.2013.06.010.

[9] B. Lauterböck, M. Nikolausz, Z. Lv, M. Baumgartner, G. Liebhard, W. Fuchs, Improvement of anaerobic digestion performance by continuous nitrogen removal with a membrane contactor treating a substrate rich in ammonia and sulfide., Bioresour. Technol. 158 (2014) 209–16. doi:10.1016/j.biortech.2014.02.012.

[10] M. Gryta, Membrane distillation of NaCl solution containing natural organic matter, J. Memb. Sci. 181 (2001) 279–287. doi:10.1016/S0376-7388(00)00582-2.

[11] L. Masse, D.I. Massé, V. Beaudette, M. Muir, Size distribution and composition of particles in raw and anaerobically digested swine manure, Trans. Am. Soc. Agric. Eng. 48 (2005) 1943–1949.

[12] R. Klaassen, P. Feron, A. Jansen, Membrane contactor applications, Desalination. 224 (2008) 81–87. doi:10.1016/j.desal.2007.02.083.

[13] B. Norddahl, V.G. Horn, M. Larsson, J.H. du Preez, K. Christensen, A membrane contactor for ammonia stripping, pilot scale experience and modeling, Desalination. 199 (2006) 172–174. doi:10.1016/j.desal.2006.03.037.

[14] M.A. Sutton, C.M. Howard, J.W. Erisman, G. Billen, A. Bleeker, P. Grennfelt, V.G. H., G. B., Nitrogen in current European policies The European Nitrogen Assessment, CAMBRIDGE UNIV PRESS, Cambridge, 2011.

[15] N. Miladinovic, L.R. Weatherley, Intensification of ammonia removal in a combined ion-exchange and nitrification column, Chem. Eng. J. 135 (2008) 15–24. doi:10.1016/j.cej.2007.02.030.

[16] T.C. Jorgensen, L.R. Weatherley, Ammonia removal from wastewater by ion exchange in the presence of organic contaminants., Water Res. 37 (2003) 1723–8. doi:10.1016/S0043-1354(02)00571-7.

[17] J. Wang, B. Fan, Z. Luan, D. Qu, X. Peng, D. Hou, Integration of direct contact membrane distillation and recirculating cooling water system for pure water production, J. Clean. Prod. 16 (2008) 1847–1855. doi:10.1016/j.jclepro.2007.12.004.

[18] S. Shirazian, A. Moghadassi, S. Moradi, Numerical simulation of mass transfer in gas–liquid hollow fiber membrane contactors for laminar flow conditions, Simul. Model. Pract. Theory. 17 (2009) 708–718. doi:10.1016/j.simpat.2008.12.002.

[19] Z. Zhu, Z. Hao, Z. Shen, J. Chen, Modified modeling of the effect of pH and viscosity on the mass transfer in hydrophobic hollow fiber membrane contactors, J. Memb. Sci. 250 (2005) 269–276. doi:10.1016/j.memsci.2004.10.031.

[20] A. Hasanoğlu, J. Romero, B. Pérez, A. Plaza, Ammonia removal from wastewater streams

through membrane contactors: Experimental and theoretical analysis of operation parameters and configuration, Chem. Eng. J. 160 (2010) 530–537. doi:10.1016/j.cej.2010.03.064.

[21] M. Rezakazemi, S. Shirazian, S.N. Ashrafizadeh, Simulation of ammonia removal from industrial wastewater streams by means of a hollow-fiber membrane contactor, Desalination. 285 (2012) 383–392. doi:10.1016/j.desal.2011.10.030.

[22] S.N. Ashrafizadeh, Z. Khorasani, Ammonia removal from aqueous solutions using hollow-fiber membrane contactors, Chem. Eng. J. 162 (2010) 242–249. doi:10.1016/j.cej.2010.05.036.

[23] E. Licon, M. Reig, P. Villanova, C. Valderrama, O. Gibert, J.L. Cortina, Ammonium removal by liquid–liquid membrane contactors in water purification process for hydrogen production, Desalin. Water Treat. 56 (2014) 3607–3616. doi:10.1080/19443994.2014.974216.

[24] A. Gabelman, S.-T. Hwang, Hollow fiber membrane contactors, J. Memb. Sci. 159 (1999) 61–106. doi:10.1016/S0376-7388(99)00040-X.

[25] E.A. Fouad, H.-J. Bart, Emulsion liquid membrane extraction of zinc by a hollow-fiber contactor, J. Memb. Sci. 307 (2008) 156–168. doi:10.1016/j.memsci.2007.09.043.

[26] D. Guaya, C. Valderrama, A. Farran, J.L. Cortina, Modification of a natural zeolite with Fe(III) for simultaneous phosphate and ammonium removal from aqueous solutions, J. Chem. Technol. Biotechnol. (2015) n/a–n/a. doi:10.1002/jctb.4763.

[27] D. Guaya, C. Valderrama, A. Farran, C. Armijos, J.L. Cortina, Simultaneous phosphate and ammonium removal from aqueous solution by a hydrated aluminum oxide modified natural zeolite, Chem. Eng. J. 271 (2015) 204–213. doi:10.1016/j.cej.2015.03.003.

[28] X. Tan, S.P. Tan, W.K. Teo, K. Li, Polyvinylidene fluoride (PVDF) hollow fibre membranes for ammonia removal from water, J. Memb. Sci. 271 (2006) 59–68. doi:10.1016/j.memsci.2005.06.057.

Appendix A. Prediction of free proton concentration

For nitric acid/ammonia solutions: The total concentration of both ammonium and ammonia ($C_{t(N)}$) at the stripping side will increase during the experiment, and the ratio between the two species will depend on the pH, as expressed in Eqs. 1A-2A:

$$C_{t(N)} = [NH_3] + [NH_4^+] = [NH_3] + \frac{C_{t(N)}}{1+10^{-\log[H^+]-pka}} \quad (1A)$$

$$[H^+] + [NH_4^+] = [NO_3^-] + [OH^-] \quad (2A)$$

Therefore, taking into account the ammonia/ammonium mass balance, the total ammonia concentration ($C_{t(N)}$) as a function of pH is expressed by Eq. 3A:

$$C_{t(N)} = \left([NO_3^-] + 10^{-\log[H^+]-14} - 10^{-\log[H^+]}\right) \cdot \left(1 + 10^{-\log[H^+]-pka}\right) \quad (3A)$$

where K_a is the NH_4^+ /NH_3 acid-base equilibrium constant, which is described by Eq. 4A:

$$NH_4^+ \leftrightarrow NH_3 + H^+ \qquad K_a = \frac{[NH_3][H^+]}{[NH_4^+]} \quad (4A)$$

For phosphoric acid/ammonia solutions: Similar to that for the nitric acid solutions, Eqs. 5A-6A describe the phosphoric mass and electroneutrality:

$$[H_3PO_4] + [H_2PO_4^-] + [HPO_4^{2-}] + [PO_4^{3-}] = C_{t(P)} \quad (5A)$$

$$[H^+] + [NH_4^+] = [H_2PO_4^-] + 2[HPO_4^{2-}] + 3[PO_4^{3-}] + [OH^-] \quad (6A)$$

Therefore, the total phosphoric acid concentration/pH dependence is expressed by Eq. 7A:

$$C_{t(P)} =$$

$$\left(1 + 10^{-\log[H^+]-pka}\right) \cdot$$

$$\left(10^{-\log[H^+]-14} - 10^{+\log[H^+]} + \frac{C_{t(P)}}{1+10^{-\log[H^+]-pka2}+10^{pka1+\log[H^+]}+10^{-2\log[H^+]-pka2-pka3}} + \right.$$

$$\frac{2C_{t(P)}}{1+10^{pka2+\log[H^+]}+10^{-\log[H^+]-pka3}+10^{pka1+pka2+2\log[H^+]}} +$$

$$\left. \frac{3C_{t(P)}}{1+10^{pka1+pka2+pka3+3\log[H^+]}+10^{pka2+pka3+2\log[H^+]}+10^{pka3+\log[H^+]}} \right) \quad (7A)$$

where K_{a1}, K_{a2} and K_{a3} are the acid-base equilibrium constants for the phosphoric system (H_3PO_4/$H_2PO_4^-$/ HPO_4^{2-}/ PO_4^{3-}) and described by Eqs. 8A-9A and 10A:

$$H_3PO_4 \leftrightarrow H_2PO_4^- + H^+ \qquad K_{a1} = \frac{[H_2PO_4^-][H^+]}{[H_3PO_4]} \tag{8A}$$

$$H_2PO_4^- \leftrightarrow HPO_4^{2-} + H^+ \qquad K_{a2} = \frac{[HPO_4^{2-}][H^+]}{[H_2PO_4^-]} \tag{9A}$$

$$HPO_4^{2-} \leftrightarrow PO_4^{3-} + H^+ \qquad K_{a3} = \frac{[PO_4^{3-}][H^+]}{[HPO_4^{2-}]} \tag{10A}$$

Annex B. Ammonia removal mechanism from concentrated NaOH solutions

Due to the high pH, only transport of ammonia gas (C_j) is considered in the lumen and expressed through a convective-diffusive equation for a single hollow fibre:

$$\frac{\partial C_j}{\partial t} + U_z \frac{\partial C_j}{\partial Z} = D_j \left[\frac{1}{r} \frac{\partial}{\partial r} \left(r \frac{\partial C_j}{\partial r} \right) + \frac{\partial^2 C_j}{\partial Z^2} \right] \tag{B1}$$

This equation is solved by taking into account laminar flow to describe the velocity profile as well as the respective boundary conditions:

The concentration in the feed tank at the inlet:

$$C_{j,Z=0} = C_{\tan k} \tag{B2}$$

Outflowing condition at the end of the fibre:

$$\left(\frac{\partial C_j}{\partial Z} \right)_{z=L} = 0 \tag{B3}$$

Symmetry at the fibre centre:

$$\left(\frac{\partial C_j}{\partial r} \right)_{r=0} = 0 \tag{B4}$$

Flux through the membrane at the fibre wall:

$$-D_j \left(\frac{\partial C_j}{\partial r} \right)_{r=r_{hf}} = k_{g,pore} \left(\frac{p^g{}_{a,\mathrm{int}1} - p^g{}_{a,\mathrm{int}2}}{R_g T} \right) \tag{B6}$$

The partial pressure of ammonia is calculated using Henry's law (Eq. S15) with the interfacial concentration of ammonia gas on both sides of the membrane. Finally, recirculation to the feed tank assuming uniform mixing is described by:

$$V\frac{dC_{\tan k}}{dt} = Q(C_{j,z=L} - C_{\tan k}) \quad \text{(B7)}$$

A more detailed description of the transport model is summarized in the Supplementary Information.

Figure captions

Figure 1. Experimental set-up of the hollow fiber LLMC including a polypropylene tank containing the feed stream (NH_3/NaOH solution) and polypropylene tank containing the nitric/phosphoric acid solution.

Figure 2. Schematic description of the ammonia transport from the feed solution through the hydrophobic hollow fiber membrane.

Figure 3. Evolution of the ammonia concentration ratio (LnC_t/C_0) as a function of time for experiments at flow rates of 10.5 and 9.1 cm^3/s at 1.2 g/L NaOH concentrates and for 0.5% HNO_3 as stripping solution.

Figure 4. Response surface of ammonia removal by HFLLC as function of initial ammonia concentration and flow rate according to the factorial experimental design (Table 1).

Figure 5. Evolution of the ammonia concentrations and pH as a function of time in a two consecutive cycles (cycle 1 from 1 to 80 minutes, and cycle to from 80 to 140) for 1.7 g/L NH_3 and 8 g/L NaOH concentrates at flow rates of 0.5 L/min and for nitric concentration of 0.5 g/L as striping phase.

Figure 6. Evolution of the ammonia concentration in the feed phase and the pH and phosphate concentration in the stripping phase as a function of time in a two consecutive cycles (cycle 1 from 1 to 80 minutes, and cycle to from 80 to 120) for 1.7 g/L NH_3 and 8 g/L NaOH concentrates at flow rates of 0.5 L/min and for an initial phosphoric acid concentration of 0.4 M as stripping phase.

Figure 7. Evolution of the ammonia concentration profile in the feed phase as a function of time for four consecutive cycles using concentrates eluted from loaded zeolites samples (1.8 to 2.7 g/L NH_3 and 1.2 g/L NaOH concentrates) at flow rates of 0.5 L/min and for an initial phosphoric acid concentration of 0.4M as stripping phase. For each feed solution a single stripping solution of acid was used.

Figure

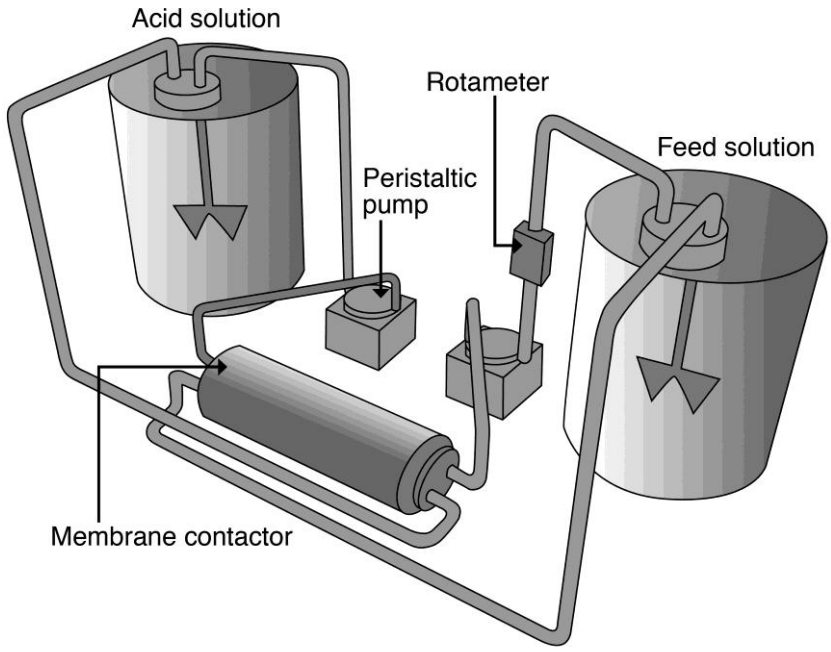

Figure 1.

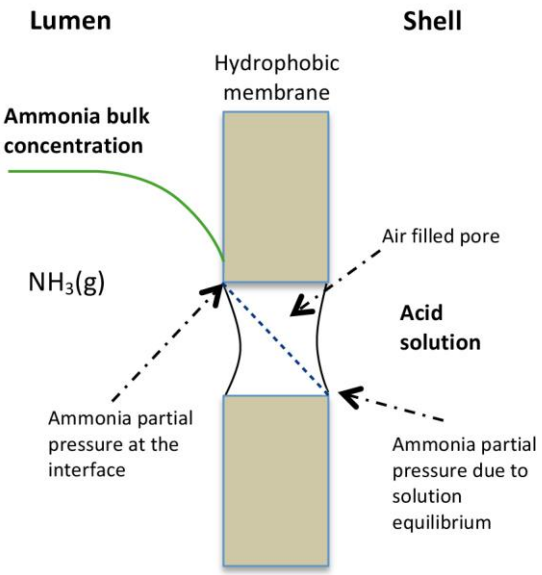
Lumen
Shell
Hydrophobic membrane
Ammonia bulk concentration
$NH_3(g)$
Air filled pore
Acid solution
Ammonia partial pressure at the interface
Ammonia partial pressure due to solution equilibrium

Figure 2.

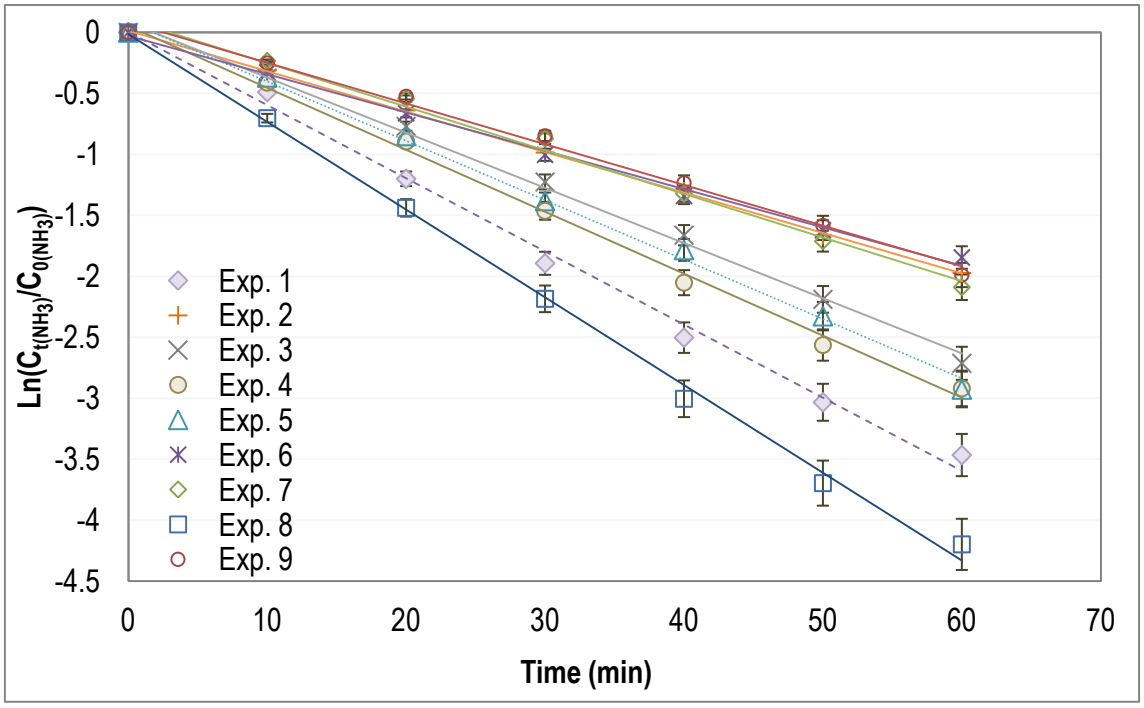
0
-0.5
-1
-1.5
-2
-2.5
-3
-3.5
-4
-4.5
0
10
20
30
40
50
60
70
Ln(C_t(NH3)/C_0(NH3))
Time (min)
Exp. 1
Exp. 2
Exp. 3
Exp. 4
Exp. 5
Exp. 6
Exp. 7
Exp. 8
Exp. 9

Figure 3.

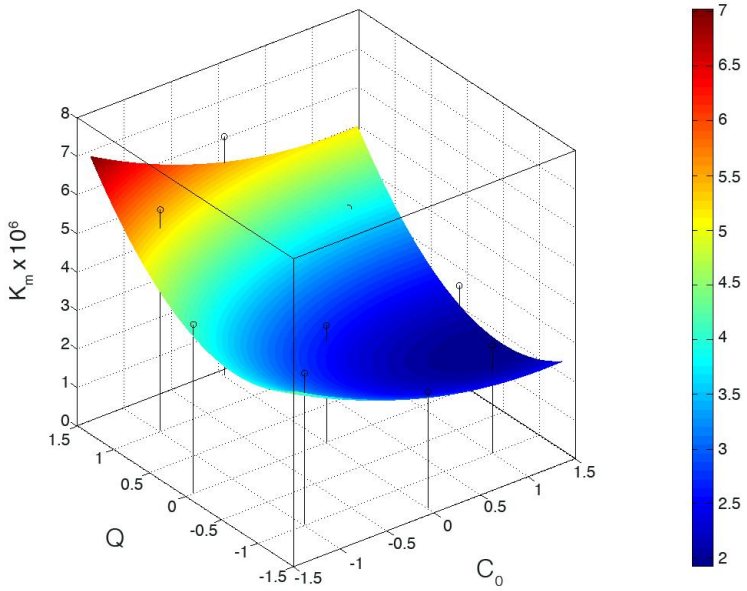
$K_m \times 10^6$
8
7
6
5
4
3
2
1
0
1.5
1
0.5
0
-0.5
-1
-1.5
Q
-1.5
-1
-0.5
0
0.5
1
1.5
C_0
7
6.5
6
5.5
5
4.5
4
3.5
3
2.5
2

Figure 4.

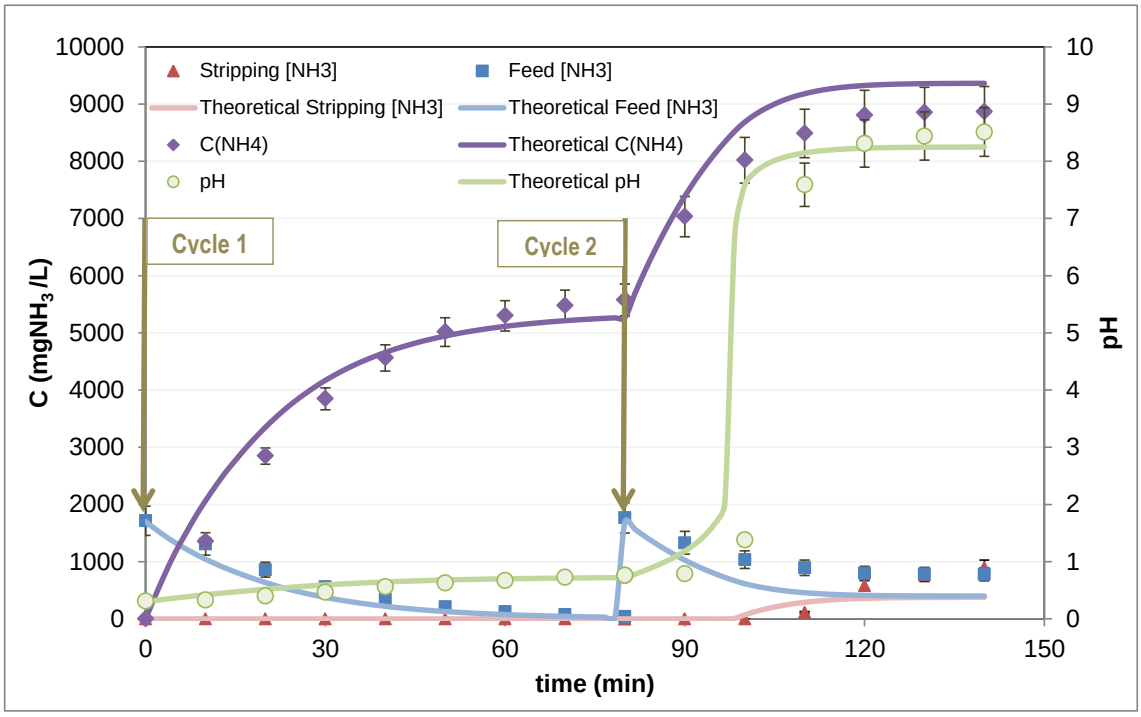
Stripping [NH3]
Feed [NH3]
Theoretical Stripping [NH3]
Theoretical Feed [NH3]
C(NH4)
Theoretical C(NH4)
pH
Theoretical pH
Cycle 1
Cycle 2
C (mgNH3/L)
pH
time (min)
0
1000
2000
3000
4000
5000
6000
7000
8000
9000
10000
0
1
2
3
4
5
6
7
8
9
10
0
30
60
90
120
150

Figure 5.

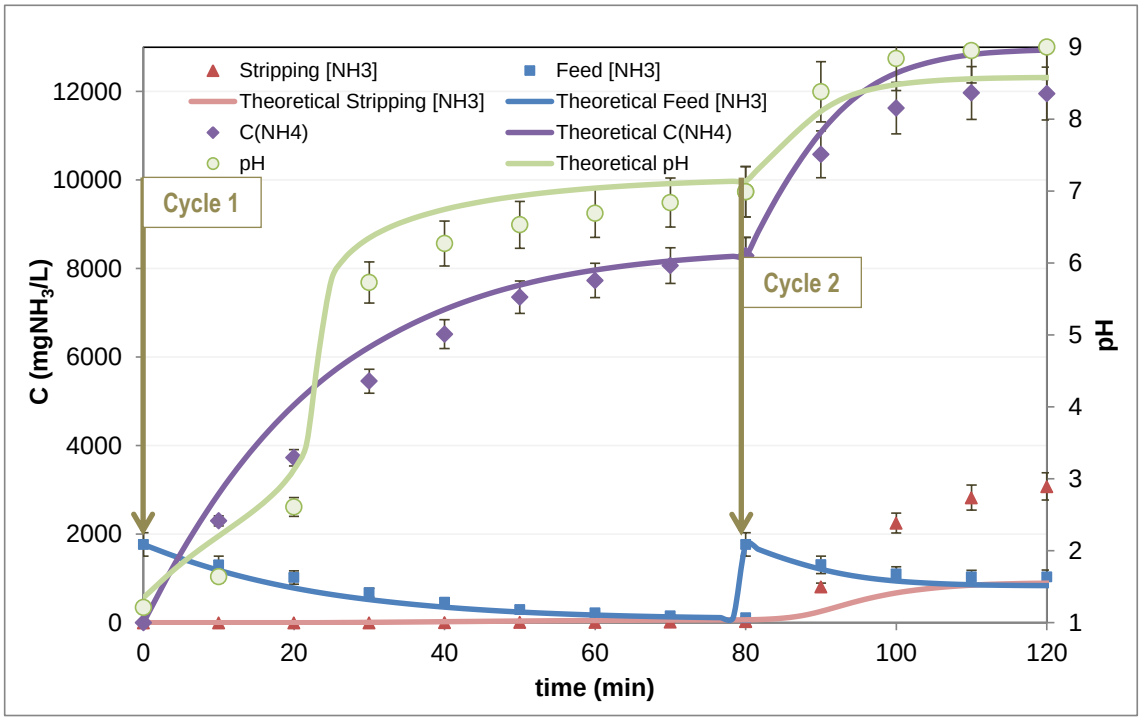
Stripping [NH3]
Feed [NH3]
Theoretical Stripping [NH3]
Theoretical Feed [NH3]
C(NH4)
Theoretical C(NH4)
pH
Theoretical pH
Cycle 1
Cycle 2
C (mgNH3/L)
pH
time (min)
0
2000
4000
6000
8000
10000
12000
1
2
3
4
5
6
7
8
9
0
20
40
60
80
100
120

Figure 6.

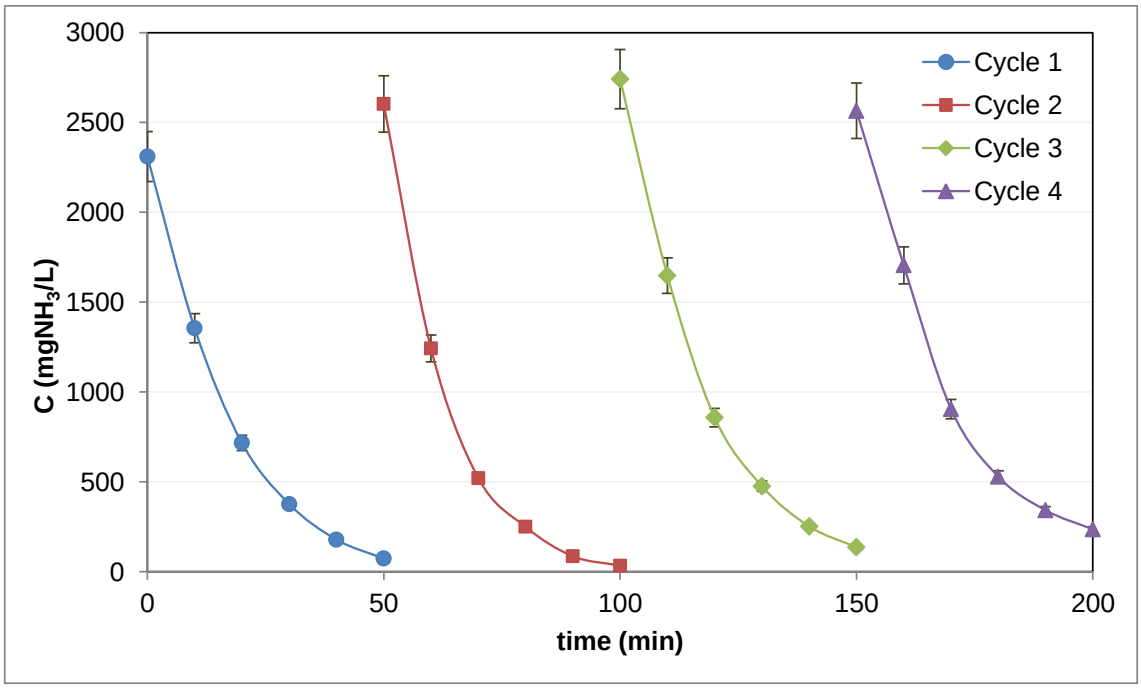
3000
2500
2000
1500
1000
500
0
C (mgNH3/L)
0
50
100
150
200
time (min)
Cycle 1
Cycle 2
Cycle 3
Cycle 4

Figure 7.